Analysis of Tornadic and Nontornadic Convective Cell Environments During Hurricane Harvey

Justin R. Spotts and Christopher J. Nowotarski
Texas A&M University, College Station, TX

Scott Overpeck
NWS Forecast Office, League City, TX

Brian Filipiak
University of Rochester, Rochester, NY

Roger Edwards
Storm Prediction Center, Norman, OK

Background

Many hazards are associated with tropical cyclones (TCs) including flooding, storm surge, and wind damage. In addition to these hazards, TCs can create environments that are favorable for the formation of miniature supercells and tropical cyclone tornadoes (TCTORs). Previous studies have indicated that there may be differences between supercell environments in TCs and their Great Plain counterparts. These include lower CAPE, higher precipitable water, lower 700-500-mb lapse rates, and lower significant tornado and supercell composite parameter values, which results in more marginal environments for TCTORs (Edwards et al. 2012). Detection of TCTORs using Next Generation Radar (NEXRAD) can be difficult, particularly at longer ranges, due to more subtle features and shallower supercells (Spratt et al. 1997). Given these challenges in the forecasting and detection of TCTORs, a comparison of environmental and radar characteristics of tornadic and nontornadic convective cells within TCs is necessary to provide to improve prediction and real-time detection of cells that may produce TCTORs.

Hurricane Harvey produced numerous TCTORs. From 25 August 2017 to 2 September 2017, Harvey produced 52 known TCTORs with approximately 326 tornado warnings. These numbers yield a ratio of TCTORs to tornado warnings of approximately 0.16. Considering that 34 of the TCTORs were warned, the false alarm ratio (FAR) for the event of was approximately 0.90. The purpose of this study is to determine which, if any, environmental and radar indices discriminate between TCTORs (ALL TOR) and tornado-warned signatures that did not produce a TCTOR (NON TOR), as well as between TCTORs that did (TOR TDS) and did not (TOR NO TDS) produce a radar-indicated tornado debris signature (TDS; Ryzhkov et al. 2005; Edwards and Picca 2016) in Hurricane Harvey.

Methods

(a) Hurricane Harvey Spatial/Temporal Domain

Before determining which tornado warnings to examine, a list of National Weather Service (NWS) County Warning Areas (CWAs) with tornadoes and warnings associated with Harvey was determined including the time period each CWA was affected. Based on McCaul (1991), a radius of 800 km from Harvey's track (Landsea and Franklin 2013) was used to identify affected CWAs. Over Harvey's lifetime, archived radar and satellite imagery (https://www2.mmm.ucar.edu/imagearchive/) was examined, starting when outer rain bands of Harvey began to pass over the contiguous United States (CONUS). The time when the bands made

landfall or 48 hours before TC landfall, whichever came first, was used as the start of the period. The same data were examined for when the bands exited CONUS, determining the end of the period. This resulted in a period of interest from 24 August 2017 at 0300Z to 4 September 2017 at 1000Z.

(b) Environment

Each affected CWA was searched for tornado warnings using the Iowa State COW (ISC) (https://mesonet.agron.iastate.edu/cow/). warnings were then checked against the ISC radar reflectivity for evidence that the convection was associated with Harvey. The qualified warnings and any subsequent updates to the warnings were then catalogued and imported to the NOAA Weather and Climate Toolkit. NEXRAD reflectivity data were then used to verify positioning of the convection of interest. Distinct areas of convection associated with a TCTOR or tornado warning are hereafter referred to as "cells." Cells that had multiple warnings issued on them with a relatively short period of time between warnings were considered "continuous." Records from the TCTOR database (Edwards 2010) were used to determine if the cell spawned a TCTOR. For each NON TOR cell, a "midpoint time" was defined halfway between the issuance of the cell's first warning and the expiration or cancellation of the cell's final warning. NEXRAD Level II and III products, including digital vertically integrated liquid, base reflectivity, and base velocity were used to subjectively determine the location of the cell at the midpoint time. For the TCTORs, midpoints between the start and endpoints of each TCTOR, along with the report time from the TCTOR database were used. The exceptions were three TCTORs that were not included due to being non-supercellular or lacking proper data. The remaining reports were then compared with radar data to ensure that the time and location were correct.

Once the midpoint times and locations of each cell and TCTOR were determined, grid point vertical profiles were obtained from the 13-km RAP model analysis for the midpoint time rounded to the nearest hour for the nearest and surrounding grid points. Each grid point was manually checked for convective contamination; if the nearest grid point appeared contaminated or had a high simulated composite reflectivity (≥ 35 dBz), the least contaminated surrounding grid point was chosen to represent that cell's inflow. The Sounding and Hodograph Analysis and Research Program in Python (SHARPpy; Blumberg et al. 2017) was used to calculate environmental indices from the RAP profiles. Profiles with a level of free convection (LFC) above 3 km were visually inspected in SHARPpy. If the LFC exceeds 3 km due to the parcel's virtual temperature cooling to or below the environmental virtual temperature near the tropopause, the profile's indices were discarded. In addition to environmental characteristics, Edwards et al. (2012) also showed that TCTORs tend to concentrate in the Northeast quadrant of the TC. As such, events from Hurricane Harvey were also binned by azimuth and range from the TC center.

(c) Radar

For this study, the radar attributes of NON TOR cells occurring in the Houston/Galveston (HGX) CWA were further analyzed using Gibson Ridge Level 2 Analyst (GR2A; http://www.grlevelx.com/gr2analyst_2/). Radar analysis for TCTOR cells from all of Harvey was included. For the NON TOR cells, only the two full volume scans leading up to and the volume including the issuance of the first warning of each cell (for a total of three volume scans) were checked for 0.5° normalized rotation (NROT) values, or if the signature was not clear, rotational velocity (VROT) values were also consulted. VROT values were calculated in

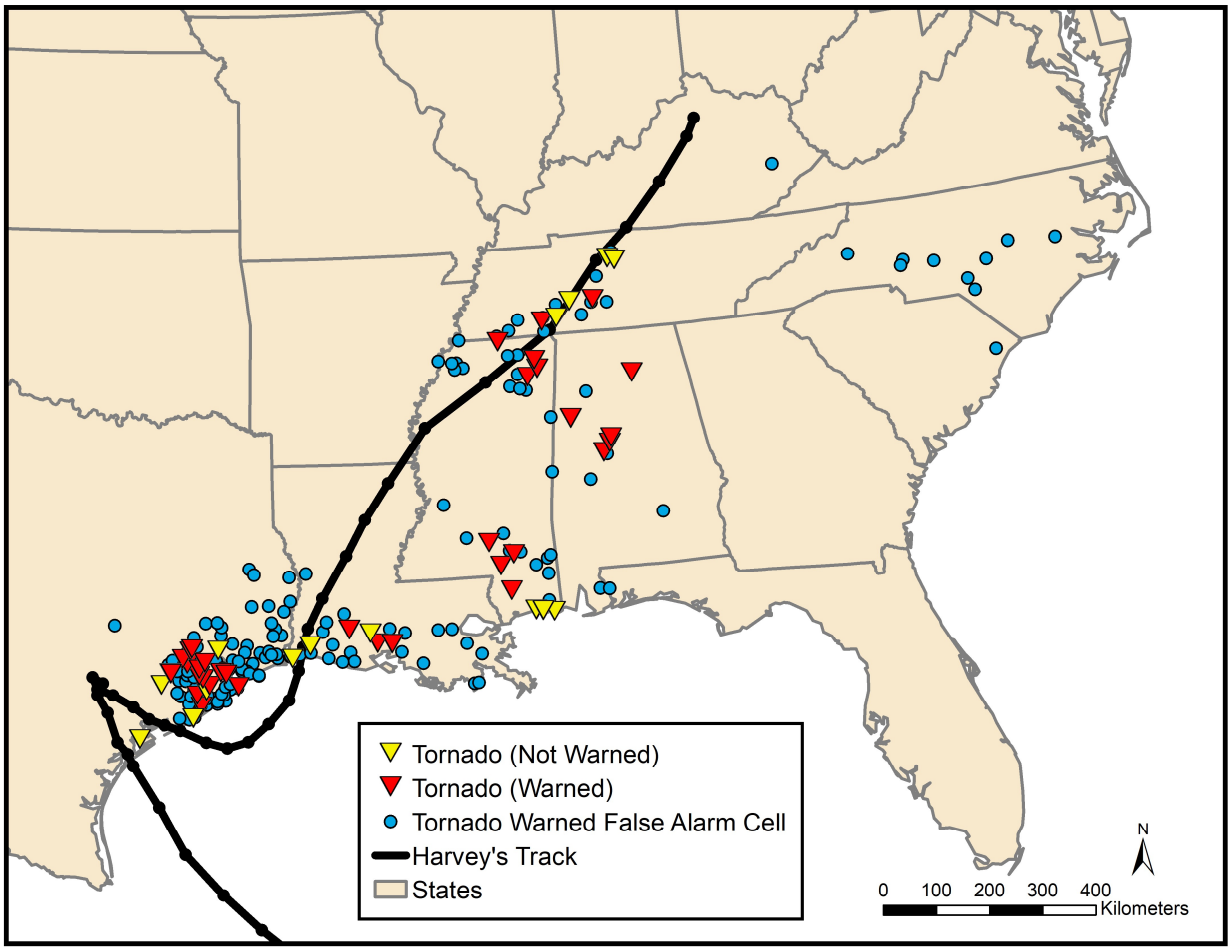

FIG 1. Overview of cases relative to Harvey's track highlight tornadic cases (warned and not warned) and the warned false alarm cells

accordance with Smith et al. (2015) with the exception that a peak radial velocity was not used if it appeared to be associated with the supercell's inflow. The full volume scan, excluding SAILS scans, with the largest 0.5° tilt NROT was used unless the rotation was noticeably over water, in which case the landfalling scan was used. Once the appropriate volume scan was selected, various radar signatures were compiled including the VROT values at the 0.5°, 0.9°, 1.3/1.5°, 1.8°, and 2.4° elevation angles if a rotational signature was present, the presence of a velocity enhancement signature (VES; Schneider and Sharp 2007), Zdr/Kdp displacement (Romine 2008; Crowe et al. 2010), and the presence of a bounded weak echo region (BWER; Spratt et al. 1997; Schneider and Sharp 2007). VROT values were only calculated at levels below 10 kft above radar level (ARL), VESs were searched for between 8 and 12 kft, and only the 0.5° tilt was examined for the Kdp/Zdr displacement and other dual-polarimetric variables. TDS signatures were evaluated according to the methods of Edwards and Picca (2016). A few NON TOR radar scans may have appeared to have false TDS signatures, but were not included because no tornado was reported. For the TCTOR categories,

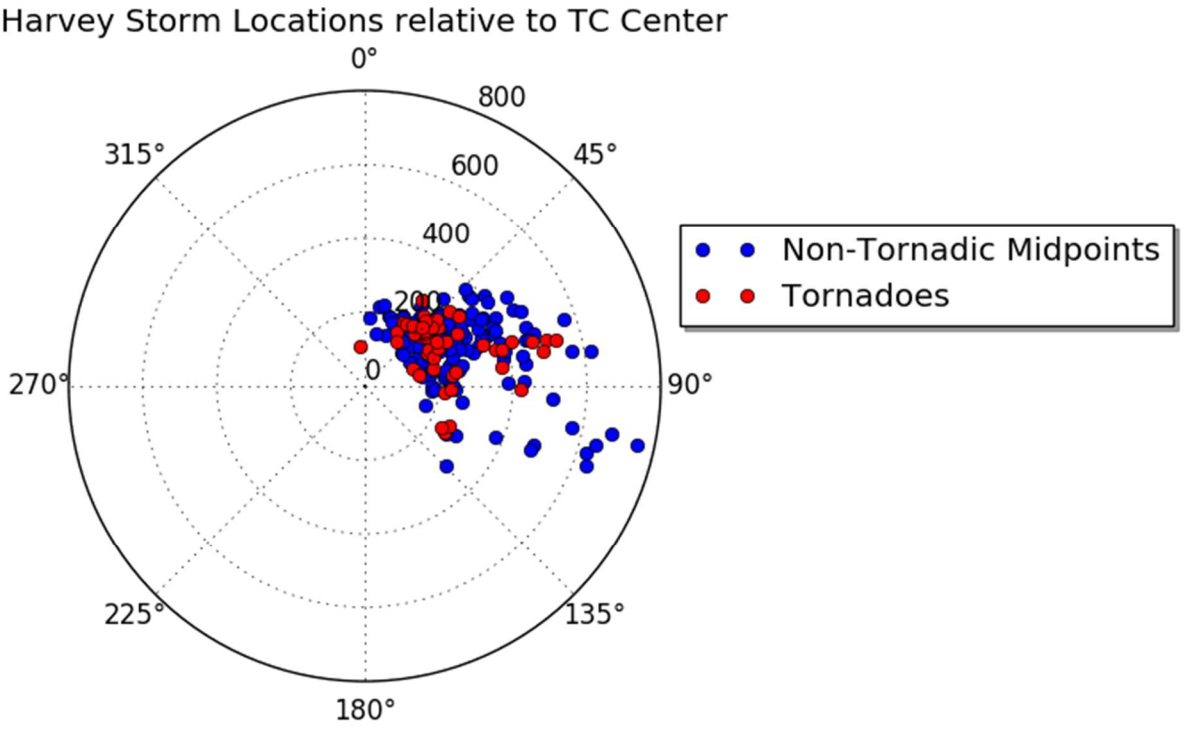

FIG. 2. Polar plot showing the locations of the ALL TOR and NON TOR categories relative to true north from the TC center.

the volume scan representative of the midpoint of the TCTOR was analyzed.

Distributions of both environmental characteristics and radar attributes were compared between cell categories to determine the best discriminators. A simple one-tailed 2-sample Z or t test was performed on noteworthy discriminators to determine if the means were significantly different ($p<0.05$; Z test if samples sizes were greater than 30, otherwise, a t-test was used). The tails tested were ALL TOR more favorable than NON TOR, TOR TDS more favorable than TOR NO TDS, and TOR NO TDS more favorable than NON TOR.

Results

(a) Spatial Distribution

When plotted on a polar plot (Fig. 2), the midpoints of the false alarm and TCTORs show that most events tend to concentrate in the northeast quadrant. This is consistent with earlier findings from Edwards et al. (2012).

(b) Environment

After qualitatively comparing 26 sounding-derived environmental parameters, the top discriminators are the magnitude of the 0-6-km bulk wind difference (6kmShear), the 0-1-km storm relative helicity (SRH1), the supercell composite parameter (SCP), the fixed layer significant tornado parameter (STPFIX), the 0-3-km lapse rate (LR3), and the 100-mb mixed layer CAPE (MLCAPE; Figs. 3-8). For the significance tests, ALL TOR has a significantly higher mean 6kmShear than the NON TOR and the TOR TDS category has a significantly higher mean than the TOR NO TDS category. TOR TDS has a significantly higher mean SRH1 than the TOR NO TDS category. For the SCP, ALL TOR has a significantly higher mean than the NON TOR category and TOR TDS has a significantly higher mean than the TOR NO TDS category. For the 0-3-km lapse rate, ALL TOR has a significantly lower mean than the NON TOR category and the TOR NO TDS has a significantly lower mean than the NON TOR category. For MLCAPE, ALL TOR has a significantly higher mean than the NON TOR category and the TOR NO TDS has a significantly higher mean than the NON TOR category. Finally, STPFIX shows statistically significant differences in all three tests.

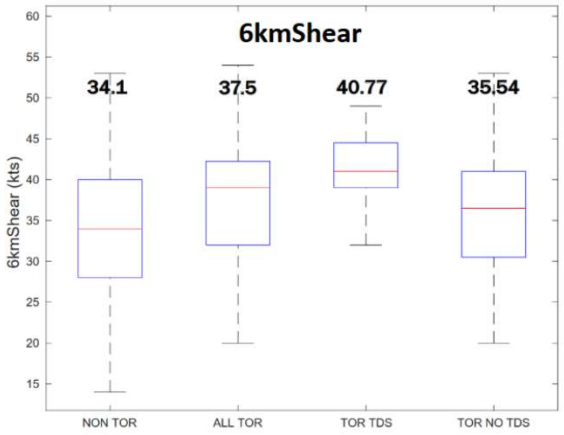

FIG. 3. Box and whisker plot of the 0-6-km shear (kts) for each category. Mean values are in bold.

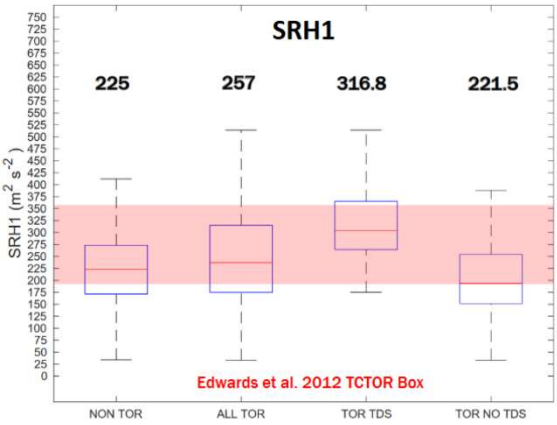

FIG. 4. Box and whisker plot of the 0-1-km right-moving storm relative helicity for each category in comparison to the inner-quartile range for TCTORs in Edwards et al. (2012; red box). Mean values are in bold.

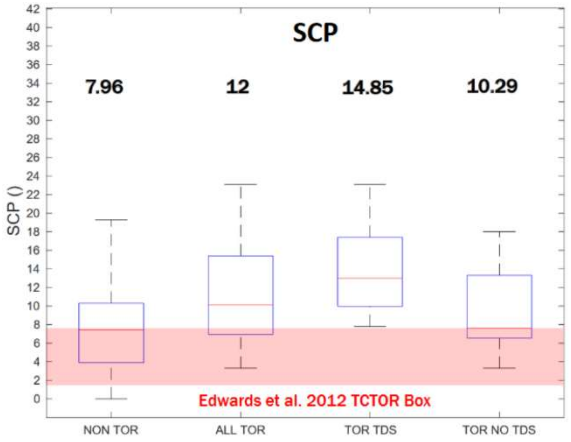

FIG. 5. As in Fig. 3, but for supercell composite parameter (SCP).

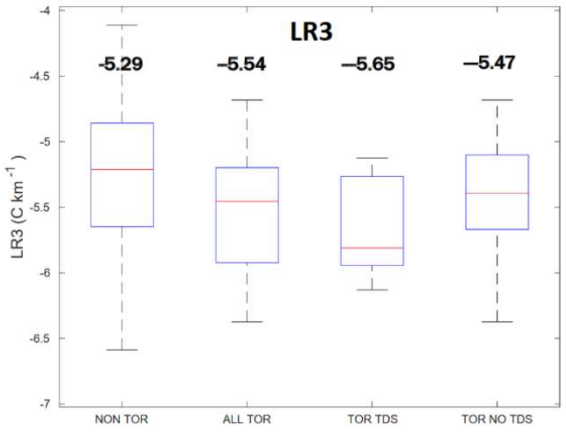

FIG. 6. As in Fig. 2, but for 0-3 km lapse rate (LR3).

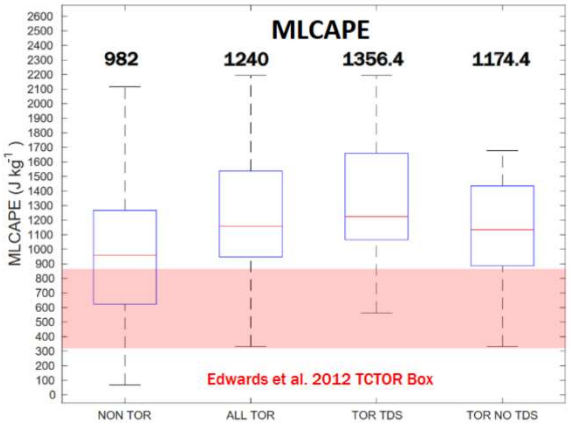

FIG. 7. As in Fig. 3, but for 100-mb mixed layer convective available potential energy (MLCAPE).

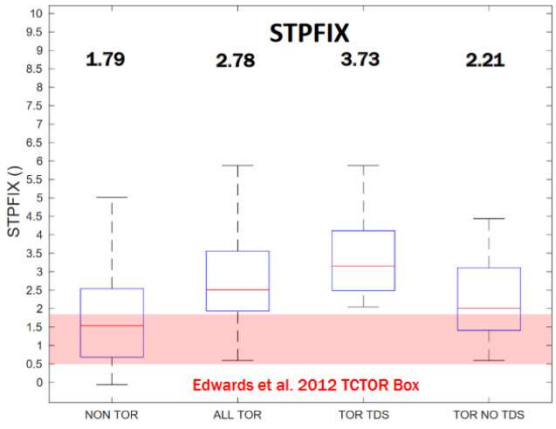

FIG. 8. As in Fig. 3, but for fixed-layer significant tornado parameter (STP).

Composite hodographs provide another perspective on which environments are more favorable for the development of updraft rotation. Figures 9 through 12 show the composite hodographs for each cell category. The ALL TOR hodograph shows a marginally more favorable profile (i.e., a longer 0-3 km hodograph) than the NON TOR hodograph. The TOR TDS also shows a more favorable hodograph than the TOR NO TDS category.

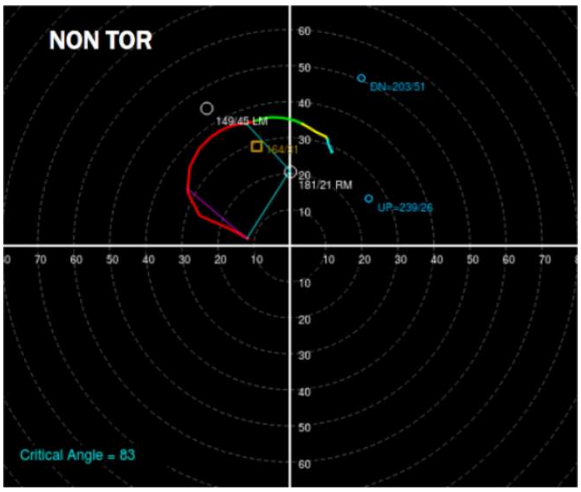

FIG. 9. Composite hodograph from all nontornadic false alarm cases (NON TOR).

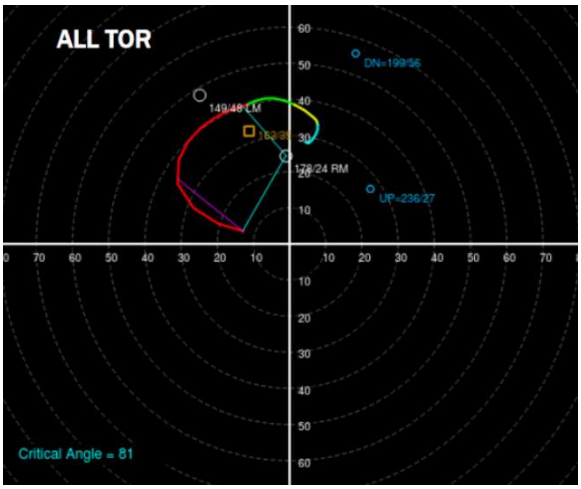

FIG. 10. Composite hodograph from all tornadic cases (ALL TOR).

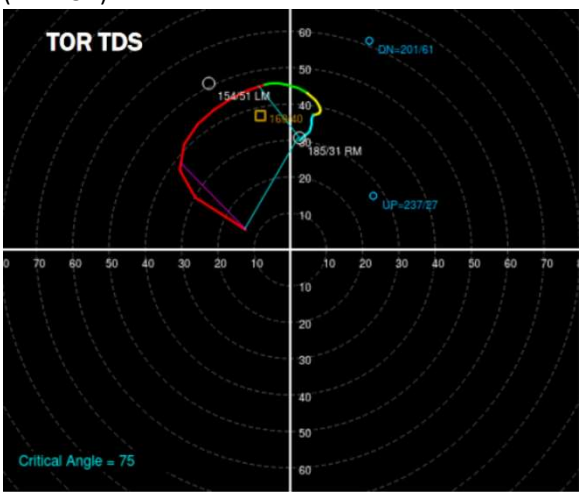

FIG. 11. Composite hodograph from all tornadic cases **with** a tornado debris signature (TOR TDS).

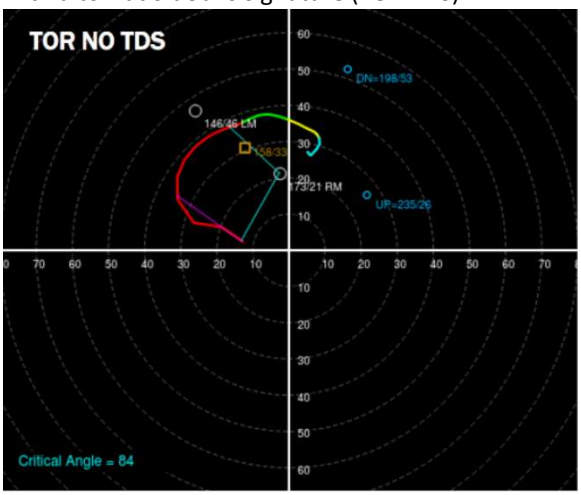

FIG. 12. Composite hodograph from all tornadic cases **without** a tornado debris signature (TOR NO TDS).

(c) Radar

The 0.5° and 2.4° VROT tilts show differences between categories as seen in Figures 13 and 14. Performing the same significance tests as the environmental indices, ALL TOR has a significantly higher mean than the NON TOR category, TOR TDS has a significantly higher mean than the TOR NO TDS category, and TOR NO TDS has a significantly higher mean than the NON TOR category for the 0.5° elevation angle. For the 2.4° elevation angle, ALL TOR cells have a significantly higher mean VROT than the NON TOR cells and the TOR NO TDS have a significantly higher mean than the NON TOR category.

The VROT values at the 0.5° and 2.4° tilts were also plotted on a scatter plot to determine if any notable trend was present in the VROT values with range from the radar in the NON TOR and ALL TOR categories as seen in Figures 15 and 16. Table 1 shows the mean values for VROT at each tilt examined where a signature was present. Other signatures which were binary (present or not present) are given as a percentage of their occurrence.

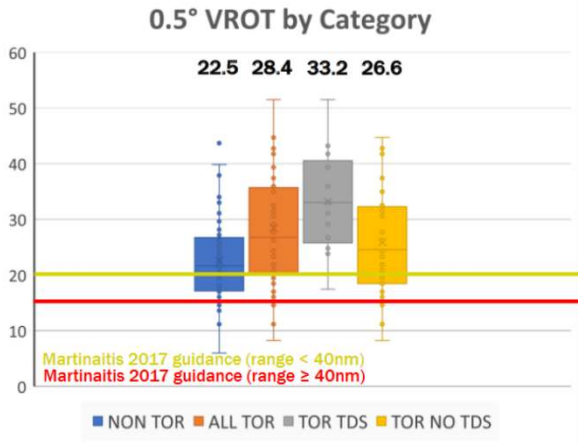

FIG. 13. Box and Whisker plot of VROT at the 0.5° tilt in comparison to the Martinaitis (2017) warning guidance (mean values in bold)

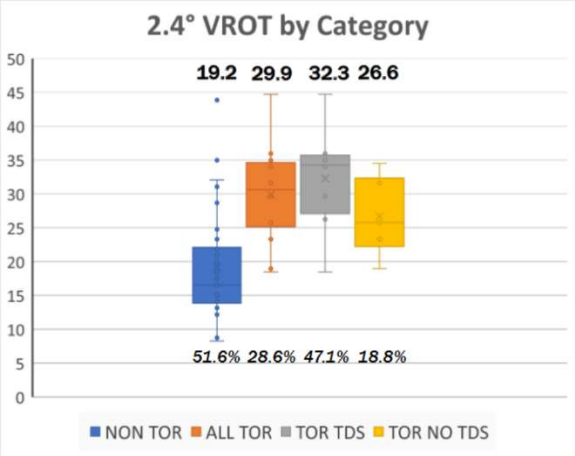

FIG. 14. Box and Whisker pot of VROT at the 2.4° tilt when the signature was present (mean values in bold. Percent of cases with the signature in italics).

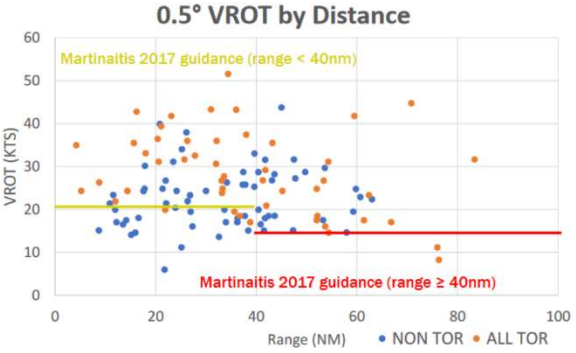

FIG. 15. Scatter plot of the 0.5° tilt VROT values for the nontornadic and tornadic cases by distance from the HGX radar in comparison to the Martinaitis (2017) warning guidance.

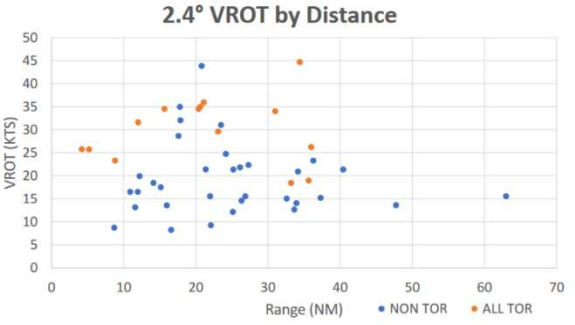

FIG. 16. Scatter plot of the 2.4° tilt VROT values for nontornadic and tornadic cases by distance from the HGX radar.

4) Conclusion

Several environmental indices showed statistically significant different means between different cell categories. While these differences in distributions can be visualized in the box and whisker plots, it should be noted that for most cases, significant overlap exists between each category. One interesting pattern that emerges from the box and whisker plots is that while there appear to be noticeable differences between the ALL TOR and NON TOR categories, those differences are far less noticeable when comparing the TOR NO TDS and NON TOR categories. Thus, the near-cell environments best identify TOR TDS cells.

When comparing Hurricane Harvey's environments to the TCTOR climatology from Edwards et al. (2012), Harvey shows higher values across all categories, even in the NON TOR cases. The exception to this SRH1, which showed values similar to the Edwards et al. (2012) TCTOR climatology across all four categories.

The radar VROT values show notable differences between categories, particularly in the 2.4° tilt ALL TOR and NON TOR categories. When comparing the 0.5° VROT values to Martinaitis (2017) guidance, VROT values were above guidance values for both ALL TOR and NON TOR categories (likely because this guidance is already part of the warning decision process). Thus, though this guidance produces a relatively high probability of detection, it is still accompanied by a high False Alarm Ratio. The analysis of VROT with distance from the radar did not reveal any notable trend. When examining the occurrence of different radar-based tornado signatures the expected pattern can be found. ALL TOR has a higher frequency of occurrence than the NON TOR category, TOR TDS has a higher frequency of occurrence than the TOR NO TDS category, and TOR NO TDS has a greater

Table 1: Number of occurrences, average VROT values, and percentage of cases with each radar signature for each category.

	NON TOR	ALL TOR	TOR TDS	TOR NO TDS
Number	64	49	17	32
0.5° VROT	11.6 m s^{-1}	14.6 m s^{-1}	17.1 m s^{-1}	13.3 m s^{-1}
0.9° VROT	10.7 m s^{-1}	14.2 m s^{-1}	17.2 m s^{-1}	12.6 m s^{-1}
1.3°/1.5° VROT	10.7 m s^{-1}	14.2 m s^{-1}	16.8 m s^{-1}	12.3 m s^{-1}
1.8° VROT	9.4 m s^{-1}	15.9 m s^{-1}	17.2 m s^{-1}	13.3 m s^{-1}
2.4° VROT	9.9 m s^{-1}	15.4 m s^{-1}	16.6 m s^{-1}	13.7 m s^{-1}
VES Occurrence	51.6%	73.5%	82.4%	68.8%
Zdr/Kdp Disp. Occurrence	23.4%	49.0%	58.8%	43.8%
BWER Occurrence	15.6%	26.5%	47.1%	15.6%
TDS Occurrence	0%	34.7%	100%	0%

than or equal frequency of occurrence than the NON TOR category. The frequencies of occurrence in each category indicate that while a TCTOR is more likely to have favorable radar signatures, such signatures also occur in false alarm cases.

Future work for this project will involve completing the environmental statistics for Hurricane Harvey and expanding the climatology to other TCs, completing the radar analysis for Hurricane Harvey and expanding to other TCs, and developing a probabilistic hazard information product based on the environmental and radar attributes for potential TCTORs.

Acknowledgements

OAA/NWS Award: NA19NWS4680007

Iowa Environmental Mesonet COW

GR2Analyst

References

Blumberg, W. G., K. T. Halbert, T. A. Supinie, P. T. Marsh, R. L. Thompson, and J. A. Hart, 2017: SHARPpy: An Open-Source Sounding Analysis Toolkit for the Atmospheric Sciences. *Bull. Amer. Meteor. Soc.*, **98**, 1625–1636, https://doi.org/10.1175/BAMS-D-15-00309.1.

Crowe, C. C., Petersen, W. A., Carey, L. D., and Cecil, D. J., 2010: A dual-polarization investigation of tornado-warned cells associated with Hurricane Rita (2005). *Electron. J. Oper. Meteor.*, **11**, http://nwafiles.nwas.org/ej/pdf/2010-EJ4.pdf.

Edwards, R., 2010: Tropical cyclone tornado records for the modernized NWS era. Preprints*, 25th Conf. on Severe Local Storms*, Denver, CO, Amer. Meteor. Soc., P3.1. https://ams.confex.com/ams/25SLS/techprogram/paper_175269.htm

Edwards, R., A. R. Dean, R.L. Thompson, and B.T. Smith, 2012: Convective Modes for Significant Severe Thunderstorms in the Contiguous United States. Part III: Tropical Cyclone Tornadoes. *Wea. Forecasting*, **27**, 1507–1519, https://doi.org/10.1175/WAF-D-11-00117.1.

Edwards, R. and J. C. Picca, 2016: Tornadic debris signatures in tropical cyclones. Preprints, *28th Conf. on Severe Local Storms*, Portland, OR, Amer. Meteor. Soc., P162.

Landsea, C. W., and J. L. Franklin, 2013: Atlantic Hurricane Database Uncertainty and Presentation of a New Database Format. *Mon. Wea. Rev.*, **141**, 3576–3592, https://doi.org/10.1175/MWR-D-12-00254.1.

Martinaitis, S.M., 2017: Radar Observations of Tornado-Warned Convection Associated with Tropical Cyclones over Florida. *Wea. Forecasting*, **32**, 165–186, https://doi.org/10.1175/WAF-D-16-0105.1.

McCaul, E.W., 1991: Buoyancy and Shear Characteristics of Hurricane-Tornado Environments. *Mon. Wea. Rev.*, **119**, 1954–1978, https://doi.org/10.1175/1520-0493(1991)119<1954:BASCOH>2.0.CO;2.

Romine, G.S., D.W. Burgess, and R.B. Wilhelmson, 2008: A Dual-Polarization-Radar-Based Assessment of the 8 May 2003 Oklahoma City Area Tornadic Supercell*. Mon. Wea. Rev.*, **136**, 2849–2870, https://doi.org/10.1175/2008MWR2330.1.

Ryzhkov, A. V., T. J. Schuur, D. W. Burgess, and D. S. Zrnić, 2005: Polarimetric tornado detection. *J. Appl. Meteor.*, **44**, 557-570, https://doi.org/10.1175/JAM2235.1.

Schneider, D. and S. Sharp, 2007: Radar Signatures of Tropical Cyclone Tornadoes in Central North Carolina. *Wea. Forecasting*, **22**, 278–286, https://doi.org/10.1175/WAF992.

Smith, B.T., R.L. Thompson, A.R. Dean, and P.T. Marsh, 2015: Diagnosing the Conditional Probability of Tornado Damage Rating Using Environmental and Radar Attributes. *Wea. Forecasting*, **30**, 914–932, https://doi.org/10.1175/WAF-D-14-00122.1.

Spratt, S.M., D.W. Sharp, P. Welsh, A. Sandrik, F. Alsheimer, and C. Paxton, 1997: A WSR-88D Assessment of Tropical Cyclone Outer Rainband Tornadoes. *Wea. Forecasting*, **12**, 479–501, https://doi.org/10.1175/1520-0434(1997)012<0479:AWAOTC>2.0.CO.